



Article

Properties of Self-Compacting Concrete (SCC) Prepared with Binary and Ternary Blended Calcined Clay and Steel Slag

Kwabena Boakye ¹ and Morteza Khorami ^{2,*}

¹ Research Institute for Clean Growth and Future Mobility, Coventry University, Coventry CV1 5FB, UK; boakyek4@uni.coventry.ac.uk

² School of Energy, Construction & Environment, College of Engineering, Environment and Science, Coventry University, Coventry CV1 5FB, UK

* Correspondence: morteza.khorami@coventry.ac.uk

Abstract: The recent emphasis on sustainable development in the construction industry has made it essential to develop construction and building materials that are not only affordable, but have minimal negative impact on the environment. This study investigates the valorisation of steel slag, which is mostly considered to be a waste material in several parts of the world, by blending with calcined impure kaolinitic clay to partially replace ordinary Portland cement (OPC) in the preparation of self-compacting concrete (SCC). OPC was substituted with steel slag at a constant level of 10%, whereas calcined clay replaced OPC at varying levels, ranging from 10 to 30% in a ternary blended mix. The hardened properties evaluated include compressive and flexural strengths. Samples containing only calcined clay showed a lower fluidity, which was significantly improved when steel slag was added to the mix. SCC containing 10% steel slag and 20% calcined clay obtained 28 days compressive strength, which was 3.6% higher than the reference cement concrete. An XRD analysis revealed a significant decrease in the peak heights of portlandite in mixtures containing steel slag and calcined clay, regardless of their replacement percentage. Generally, all the blended cement samples performed appreciably in resisting sulphate attack. The results of this study demonstrate that using steel slag and calcined clay together can significantly improve the fresh and hardened properties of SCC without compromising its mechanical properties.



Citation: Boakye, K.; Khorami, M. Properties of Self-Compacting Concrete (SCC) Prepared with Binary and Ternary Blended Calcined Clay and Steel Slag. *Infrastructures* **2024**, *9*, 46. <https://doi.org/10.3390/infrastructures9030046>

Academic Editor: Md. Safiuddin

Received: 7 January 2024

Revised: 19 February 2024

Accepted: 26 February 2024

Published: 1 March 2024



Copyright: © 2024 by the authors. Licensee MDPI, Basel, Switzerland. This article is an open access article distributed under the terms and conditions of the Creative Commons Attribution (CC BY) license (<https://creativecommons.org/licenses/by/4.0/>).

Keywords: steel slag; calcined clay; self-compacting concrete (SCC); compressive strength; flexural strength; chloride ingress

1. Introduction

Many kinds of concrete have been developed over the years aimed at expanding the construction industry and coming up with solutions to several industry-related problems, while combating environmental issues. One such intervention is self-compacting concrete (SCC), which is known for its high performance and ability to flow and compact, utilising its own weight without the use of extra vibrators [1]. The properties of SCC, such as fluidity, stability, and flowing ability, make it preferable to other types of concrete [2]. Other benefits include a relatively lower cost, shorter production time, ease of placing in restricted areas due to its flowability, and ease of casting complex designs [3].

Due to these advantages, SCC has favoured the construction of high-rise structures, dams, bridges, and several infrastructural projects [4]. With advancements in the building sector and a consequent increase in the need for construction materials such as cement and fine aggregate, the use of supplementary cementitious materials (SCMs) is quickly gaining popularity [5]. Sustainability is being impacted by the increased use of traditional building materials such as Portland cement [5,6]. Cement production is, for example, generating about 7–8% of global CO₂ emissions, while the high demand for concrete has contributed to the depletion of natural resources like aggregates and water [7]. It is, therefore, necessary to

find replacements for these materials in order to lessen the construction industry's reliance on them.

However, SCC, just like many other types of concrete, utilizes Portland cement, which is known to be unfriendly to the environment [8]. Therefore, the development of new environmentally friendly materials with the pozzolanic property that can be used as substitutes for Portland cement in concrete must be pursued to protect the global atmosphere from the effects of cement production [9]. To deal with the thorny issue of the greenhouse effect and global warming, the construction industry has welcomed the use of SCMs as partial substitutes for cement in concrete. Industrial and agricultural by-products, which, ordinarily, would be discarded as waste, have been recycled, valorised, and utilised as alternative binders in cementitious systems. Examples of such materials include steel slag, rice husk ash, fly ash, coconut shell ash, waste granite, silica fume, AND calcined clays, etc.

Kaolinitic clays, when calcined between 600 °C and 900 °C, have been found to be reactive due to their crystallinity and ordered structure [10,11]. The strength development of calcined clay blended cements is dependent on the interaction of the metakaolinite phase with portlandite to form calcium silicate hydrates and the reaction between metakaolinite with sulphate ions to generate the calcium aluminate hydrate phase [12]. It has been discovered that the incorporation of calcined clays in concrete reduces porosity and the diffusion of dangerous chemicals that accompanies it [13]. It has been proven that the kaolinite content and individual surface areas of calcined clays influence its reactivity. High-grade kaolinitic clays, however, have already discovered more lucrative uses in fields like the paper industry and refractories, rendering them expensive for concrete applications [14].

Several researchers [15–18] have, therefore, considered the potential use of low-grade clays as a cementitious material and have reported varying outcomes. Clays with a low amount of kaolinite are, however, known to compromise strength development due to poor pozzolanic reactivity. Therefore, to achieve the desired mechanical properties, a fair balance needs to be drawn between the kaolinite composition and cement substitution percentages [19]. Another way to maintain an appreciable level of mechanical characteristics without compromising durability properties is to uniformly mix with a known SCM in ternary blends to activate its synergistic advantages.

Steel slag production is rising yearly due to the growth of the steel industry. Along with taking up a lot of land area, it also emits pollutants into the atmosphere, pollutes water bodies, and produces hazardous waste [20]. The removal of steel slag waste is costing the steel industry more and more money. Large quantities of carbon powder and limestone are introduced during the reduction stage of the arc-furnace steelmaking process. These materials interact with the oxides to remove any excess oxygen in the molten steel and leave reduced slag as the byproduct. Steel slag removal uses up a lot of natural resources in the numerous waste treatment procedures, in addition to seriously polluting the air and water [21].

In recent years, extensive research has been carried out on the alternative use of steel slag as a supplementary cementitious material in concrete. Some investigators have reported an increase in fluidity and workability with the inclusion of steel slag as a partial replacement for cement in concrete [22–24]. Studies conducted by Wang et al. [25] suggested a decrease in compressive strength as the steel slag content in the cement matrix increased from 0% to 45% at curing ages of 3, 7, 28, 90, and 365 days. Other reports also showed a reduction only at early ages and an appreciation of compressive strength as the curing period was extended to 28 and 90 days for 10% and 20% replacements. Chloride penetration was observed to decrease up to 40% with steel slag replacement [26].

The research gap in the utilization of ternary blended steel slag and calcined clay for concrete lies in the limited exploration of their combined potential as supplementary cementitious materials despite their individual benefits. While both steel slag and calcined clay have been individually investigated as alternative materials in concrete production, there is a lack of comprehensive research focusing on their synergistic effects when used to-

gether in concrete mixtures., especially in SCC. Investigating the ternary blend of steel slag, calcined clay, and Portland cement in concrete formulations could lead to the development of high-performance, environmentally friendly concrete with optimized mechanical properties, durability, and sustainability [27–29]. In order to mass produce and promote such a cementitious system for construction applications, there is a need to accumulate data that would effectively support the future adoption of this sustainable binder system. This work, therefore, studied and reported on the effect of these SCMs, in varying compositions, on the rheological characteristics of SCC. The hydration, compressive strength, flexural strength, and some durability properties such as chloride permeability and sulphate resistance were evaluated and reported. The findings were referenced to ordinary Portland cement. The outcome of this work suggests that a ternary binder system comprising low-reactive calcined clay and steel slag could be used for construction without compromising the major properties of SCC.

2. Experimental Study

2.1. Materials

EN 197-1 [30] CEM I (grade 52.5) Portland cement with a specific gravity of 3.08 g/cm³ and BET specific surface area of 375 m²/kg was used in the preparation of the concrete mixtures. Low-grade clay with a kaolinite content of 19% was calcined at 800 °C for 1 h at a heating rate of 20 °C/min. It was cooled to ambient temperature in the open air for approximately 1 h. The calcined clay was milled and sieved through a 75 µm sieve. Pulverized steel slag (SS) with a specific gravity of 2.5 g/cm³ was obtained from local suppliers. The chemical compositions of the cement, calcined clay, and steel slag are shown in Table 1. The XRD spectra of the calcined clay and steel slag are presented in Figure 1. The SEM images of the calcined clay and steel slag reveal rough and irregular surface particles, as shown in Figures 2 and 3, respectively. For the concrete mixes, an uncrushed aggregate with a maximum particle size of 10 mm was used. The specific gravity, crushing value, and water absorption of the coarse aggregate were 2.55 g/cm³, 24.6%, and 0.5, respectively. Sharp sand with particles less than 5 mm and a moisture content of 0.5% served as fine aggregates for the concrete preparation.

Table 1. Chemical composition of cement, steel slag, and calcined clay.

Composition, %	SiO ₂	Al ₂ O ₃	Fe ₂ O ₃	MgO	CaO	Na ₂ O	K ₂ O	MnO	TiO ₂	P ₂ O ₅	Cl	SO ₃	LOI
Calcined clay	63.52	17.89	12.75	1.54	0.31	0.02	1.69	0.46	0.34	0.01	–	0.13	1.34
Steel slag	10.51	2.12	25.8	6.86	42.89	0.62	0.12	4.37	0.63	0.31	–	0.12	5.65
OPC	17.56	3.05	3.84	2.05	60.24	4.05	2.31	0.13	0.15	0.21	0.02	4.68	1.71

2.2. Mix Design and Casting

Mixtures of SCC containing different proportions of steel slag and calcined clay were prepared to determine their effect on fresh and hardened properties. The first set comprised the reference concrete, containing only cement as the binder and labelled as 0SS0CC. The second set of SCC was prepared using 10%, 20%, 30%, and 40% by weight of calcined clay and was labelled 10CC, 20CC, 30CC, and 40CC respectively. The last set contained a ternary mix of steel slag and calcined clay, 10% steel slag and 10% calcined clay (10SS10CC), 10% steel slag and 15% calcined clay (10SS15CC), 10% steel slag and 20% calcined clay (10SS20CC), 10% steel slag and 25% calcined clay (10SS25CC), and 10% steel slag and 30% calcined clay (10SS30CC). A constant water-to-binder ratio and superplasticiser (Auracast 400) dosage of 0.5 and 1%, respectively, were used in all mixtures. The details of the mixture proportions are presented in Table 2. The different constituents of the SCC were mixed using a laboratory-type rotary mixer. A slurry comprising cement, steel slag, and calcined clay was firstly prepared, after which, the fine and coarse aggregates were added and allowed to mix for 5 min. The fresh properties of the concrete were determined before

casting into steel moulds. The cast samples were left in open air at room temperature for 24 h before they were demoulded and cured under a pond of water for specific ages.

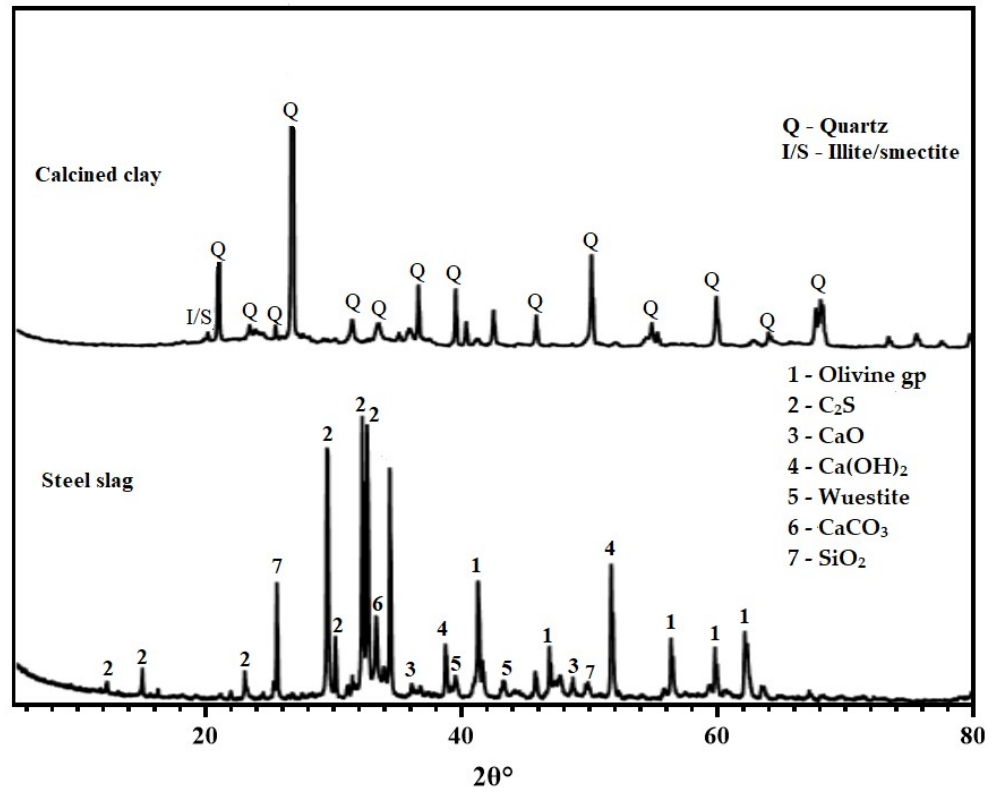


Figure 1. XRD of steel slag and calcined clay.

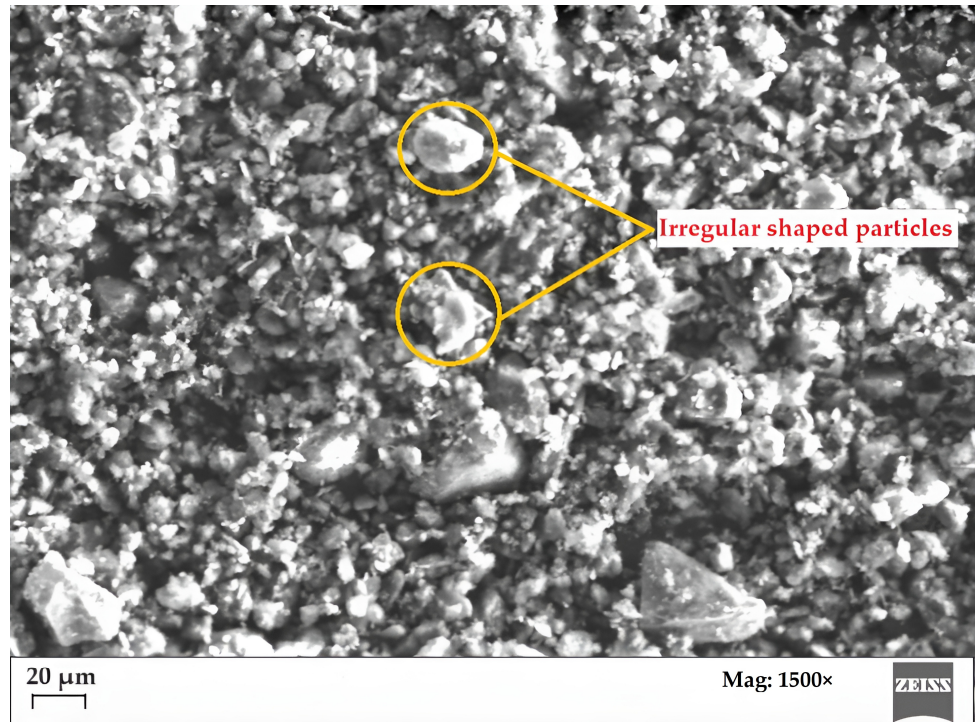


Figure 2. SEM image of calcined clay.

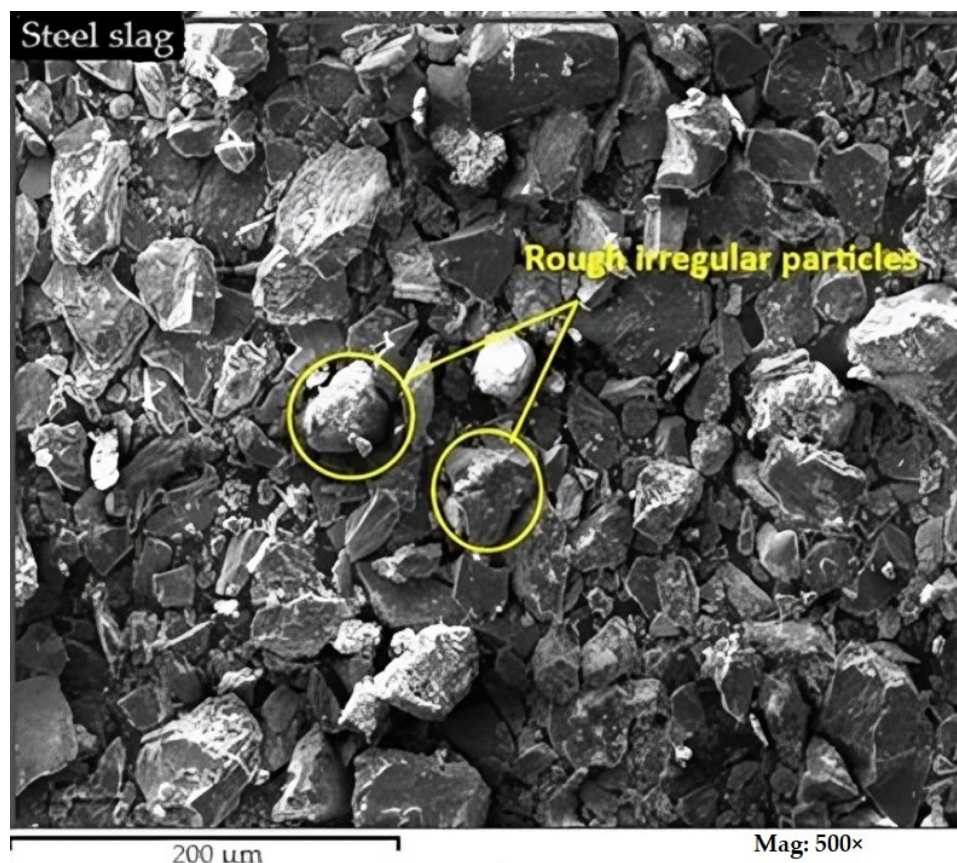


Figure 3. SEM image of steel slag.

Table 2. Mix proportion of SCC.

Mix ID	Cement, kg/m ³	SS, kg/m ³	Calcined Clay, kg/m ³	Sand, kg/m ³	CA, kg/m ³	Superplasticizer, %
0SS0CC	600	0	0	1050	900	1
10CC	540	0	60	1050	900	1
20CC	480	0	120	1050	900	1
30CC	420	0	180	1050	900	1
40CC	360	0	240	1050	900	1
10SS10CC	480	60	60	1050	900	1
10SS15CC	450	60	90	1050	900	1
10SS20CC	420	60	120	1050	900	1
10SS25CC	390	60	150	1050	900	1
10SS30CC	360	60	180	1050	900	1

2.3. Testing Methods

The fresh SCC properties such as slump flow diameter, L-box test, V-funnel test, J-ring test, and T50 flow test were determined with reference to the guidelines provided by the European Federation of National Associations Representing for Concrete (EFNARC) [31]. For the slump flow test, a slump cone was filled with fresh concrete and compacted using the tamping rod. The cone was lifted vertically upwards, allowing the SCC to flow and spread freely. The slump flow diameter was measured using a ruler. The same concrete specification was prepared and used to fill the V-funnel to the brim without applying any external force. The stopper was open at the bottom of the funnel to allow the concrete to flow freely. The time taken for the V-funnel to be completely empty was recorded. To evaluate the workability using J-ring, the slump cone was placed in the middle of the J-ring filled with fresh concrete. The cone was lifted vertically to allow the concrete to

flow freely. The extent of concrete flow was measured. The L-box consisted of two vertical arms forming an L-shape, with a horizontal plate at the junction. SCC was poured into one side of the L-box until it was full. The horizontal plate was lifted, allowing the SCC to flow through the gap to fill the other side of the box. The distance travelled by the SCC along the horizontal plate was measured. The T50 test apparatus consisted of a truncated cone-shaped mould with a diameter of 50 mm at the top and a height of 180 mm. The cone was filled with SCC and lifted vertically. The diameter of the concrete spread at the top of the mould after the cone was removed was measured. The compressive strength was tested using $100 \times 100 \times 100$ mm concrete cubes using procedures recommended by ASTM C109 [32]. A flexural strength test was carried out with reference to ASTM C78 [33]. The fresh concrete was placed in the moulds in three layers and tamped after each layer. It was left to cure for 24 h before demoulding and was cured under water until the compressive and flexural strength testing day. For the sulphate resistance test, concrete specimens, after curing, were immersed in a 5% Na_2SO_4 solution for a period of 90 days, and the effect of the Na_2SO_4 on the SCC was evaluated according to the weight loss and compressive strength. To study the hydration products, portions of the SCC, after the compressive strength test, were chipped, ground to a fine powder, and tested using the XRD technique. The rapid chloride permeability test (RCPT), recommended by ASTM C1202 [34], was used to determine the susceptibility of the SCC to chloride ingress. Then, 50 mm thick slices of 100 mm diameter concrete cores were subjected to electrical current measurements over a six-hour period. One sample was submerged in a NaCl_2 solution, and the other in a NaOH solution. The ends of the specimen were kept at a potential difference of a 60 V direct current. Measurements of the current were recorded at regular intervals. The permeability of the concrete to chloride ions was determined based on the measured electrical conductivity.

3. Results and Discussion

3.1. Fresh SCC Properties

3.1.1. Slump Flow of SCC

The slump flow results of the SCC with varying compositions of calcined clay and steel slag are illustrated in Figure 4. From the results, all the slump values obtained were found between 550 and 745 mm, which are within the acceptable limit, as prescribed by EFNARC [31]. The highest slump flow diameter was recorded for the reference concrete at 745 mm, whereas the lowest was obtained for the concrete containing 40% calcined clay (550 mm). The slump flow diameter was observed to decrease steadily with an increasing calcined clay content. At 40% replacement with calcined clay (40CC), the slump flow diameter was reduced by 26.2%. This trend of a decreasing slump flow diameter was due to the amorphous nature of the calcined clay particles with a relatively higher surface area, which improved the cohesiveness of the concrete and ultimately reduced the slump flow diameter [35]. The introduction of steel slag into the mixture caused a slight stabilisation of the slump flow diameter for the samples containing 10%, 15%, and 20% calcined clay (730 mm, 740 mm, and 735 mm respectively). Beyond 20% calcined clay, the slump flow diameter declined. It is, however, worth noting that the slump flow diameter improved more in the samples with steel slag than the samples without. This is because the content of calcined clay at this stage was far more than that of steel slag, which had a relatively lower surface area, which has been confirmed by previous researchers [36,37].

3.1.2. V-Funnel and T-50 Flow Time of SCC

The V-funnel test was performed to determine the viscosity of the self-compacting concrete. It indicates how long it takes for the concrete to flow out of the V-shaped funnel. A higher V-funnel time is an indication of a high viscosity and low flowability. The T-50 flow time test, on the other hand, measures the time taken for the wet concrete to travel to the edge of the 50 cm diameter circle after removing the slump cone. These two tests were conducted to determine the viscosity and filling ability of the fresh concrete by recording

the overall flow time. Figure 5 presents the results of the V-funnel and T-50 tests. It was observed that the T-50 and V-funnel flow times significantly increased with increasing percentages of calcined clay in the concrete matrix up to 40% replacement. The V-funnel flow time for all mixtures ranged between 8.2 s (recorded for 0SS0CC) and 14.5 s (recorded for 40CC). The T-50 time also followed a similar trend, with the reference sample and 40CC obtaining the least and highest T-50 times, respectively. The addition of 10% steel slag into the mix did not have a significant impact on the fluidity of the concrete in the both the V-funnel and T-50 times. Studies conducted by other researchers [38,39] have concluded that the rise in V-funnel and T-50 flow times is due to the fine surface particles of the calcined clay, which fill the voids between larger aggregates more effectively and result in a denser packing structure.

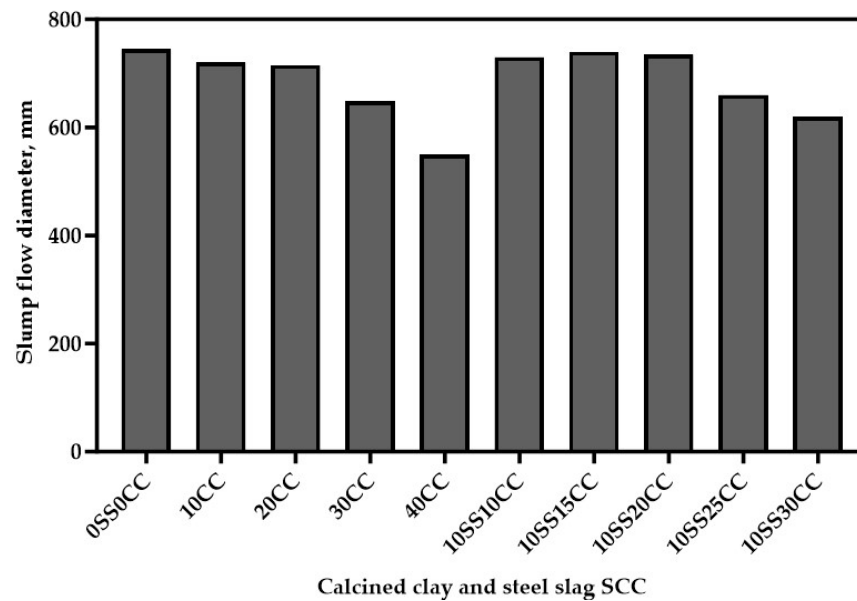


Figure 4. Slump flow of SCC with varying contents of calcined clay and steel slag.

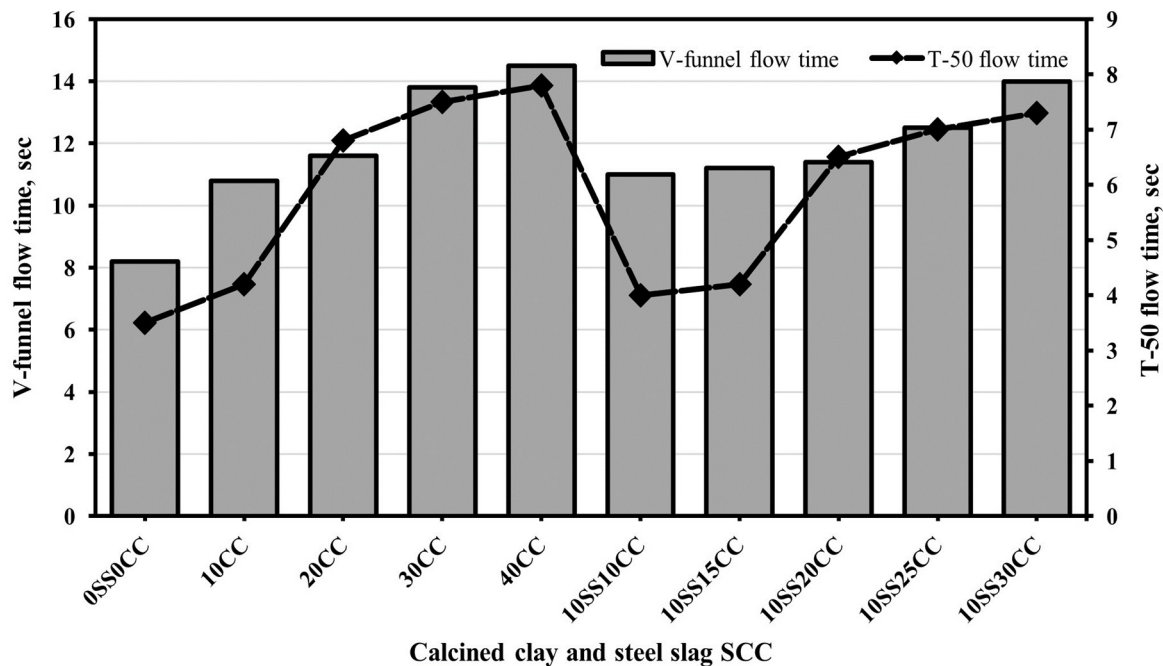


Figure 5. V-funnel and T-50 flow of SCC with varying calcined clay and steel slag content.

3.1.3. L-Box Blocking Ratio and J-Ring Test

The L-box blocking ratio (H_2/H_1) measures the ratio of the height of fresh concrete occupying the horizontal portion (H_2) to that of the vertical portion of the apparatus (H_1), whereas the J-ring measures the difference in the height of the fresh concrete in and outside the J-ring bar. The two experiments were conducted with reference to the standards prescribed by EFNARC to ascertain the concrete’s capacity to pass through reinforcement bars. The results obtained for the L-box and J-ring tests are presented in Figure 6. The results showed increasing J-ring values as calcined clay increased from 0 to 40% in the concrete matrix. Equal quantities of steel slag and calcined clay in the mixture (10SS10CC) recorded a relatively lower J-ring value. There was, however, an increase again when the calcined clay content increased from 10% to 15%, 20%, 25%, and 30%. The reference sample obtained the lowest, while the specimen containing 40% calcined clay replacement obtained the highest. This was because the addition of calcined clay can lead to an increase in yield stress, which is the minimum stress required to initiate flow. The addition of calcined clay alters the rheological behaviour of the paste by increasing its viscosity and yield stress. As a result, the concrete mixture becomes more resistant to flow, leading to longer V-funnel and T-50 flow times. Therefore, the greater the replacement, the less likely the concrete will flow at a constant water-to-cement ratio. These effects are similar to the findings of some past investigators [40,41].

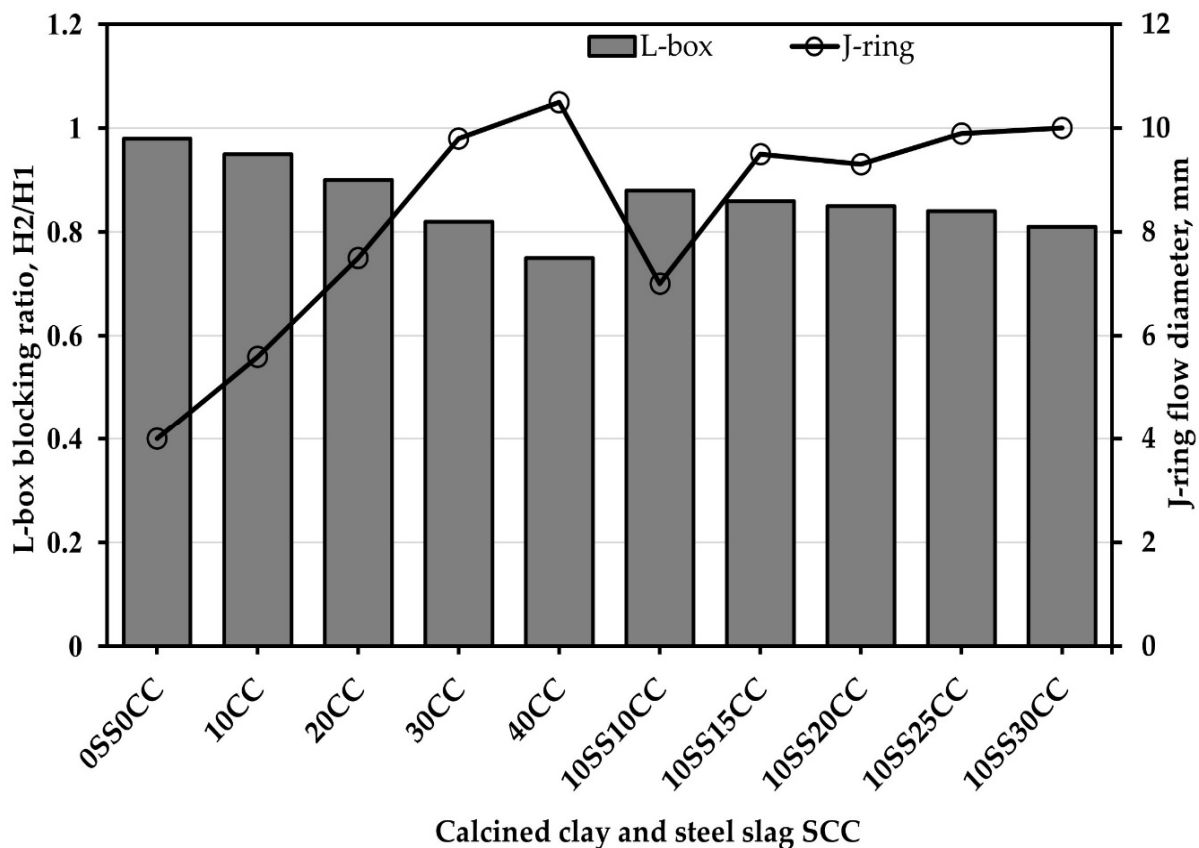


Figure 6. L-box blocking ratio and J-ring flow diameter of SCC.

All blends, in sum, demonstrated an appreciable consistency and workability. Steel slag demonstrated its capacity to make up for the loss of fluidity associated with the addition of calcined clay. The mixtures comprising 10% steel slag and 10% or 15% calcined clay as Portland cement replacements appeared to be the optimum combination to achieve satisfactory fresh SCC properties.

3.2. Hardened SCC Properties

3.2.1. Compressive Strength of SCC

Figure 7 illustrates how varying levels of cement replacement with calcined clay and steel slag influenced the 7- and 28-day compressive strength of SCC. The results indicated a consistent decrease in strength as the replacement percentage of calcined clay increased up to 40% in the mixture at both curing ages. For instance, the 7-day strength of the reference specimen was 43.55 MPa. However, this decreased by 8.7%, 19.6%, 28.9%, and 44.7%, respectively, when 10%, 20%, 30%, and 40% of the cement was replaced by calcined clay. This was due to the slow reaction between the calcined clay and the constituents of the cement, especially at early ages. The initial reactivity of pozzolans is known to be slow during preliminary stages but accelerates with time at 28 days and beyond, thereby improving strength [42]. A similar downward trend of compressive strength was reported by Dixit et al. [43], when cement was partially substituted by calcined marine clay and cured for 1, 7, and 28 days.

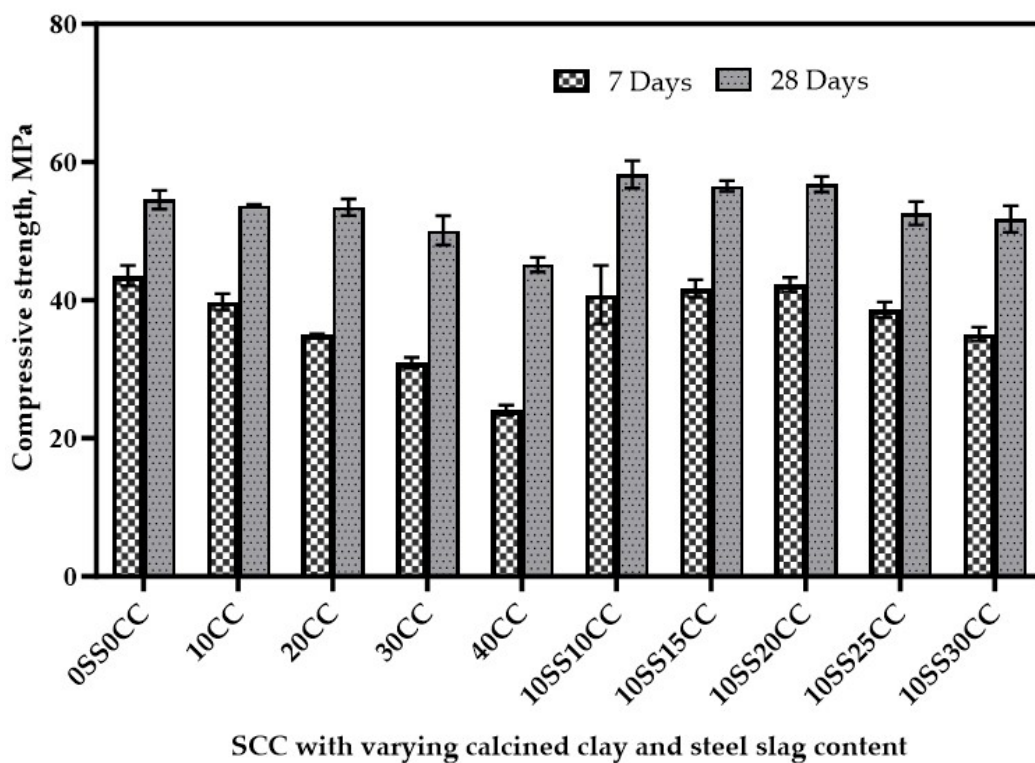


Figure 7. Compressive strength of SCC.

The trend in compressive strength development, however, changed when a constant content (10%) of steel slag was introduced as a base pozzolan in the concrete mixture. The compressive strength values obtained at 7 days for 10SS10CC, 10SS15CC, 10SS20CC, and 10SS25CC were 40.8 MPa, 41.7 MPa, 42.3 MPa, 38.6 MPa, and 35.1 MPa, respectively. With the addition of steel slag, the compressive strength at 7 days was observed to increase with an increasing calcined clay content up to 20%. Beyond 20% calcined clay, the compressive strength suffered a decline. At 28 days, 10SS10CC, 10SS15CC, and 10SS20CC obtained compressive strengths of 58.2 MPa, 56.6 MPa, and 56.6 MPa, which are about 6.2%, 3.5%, and 3.9% higher than the reference sample. The compressive strength improvement in these mixtures was linked to the fine surface particle sizes of steel slag in comparison to the calcined clay, which led to refinement of the pore sizes and packing density [44]. Other researchers have attributed the rise in compressive strength to the active interaction between the steel slag and calcined clay constituents to facilitate the production of calcium silicate hydrates, responsible for the development of strength [45–48]. However, as the

calcined clay content increased in 10SS25CC and 10SS30CC, the compressive strength declined due to the dilution effect and its consequential effect of portlandite consumption. Substitution of the cement component with calcined clay diluted the overall cementitious content in the concrete mixture, leading to a decrease in the hydration products (calcium silicate hydrates) formed during the curing process. Consequently, the development of intermolecular bonds and the overall strength of the concrete were adversely affected. A similar trend of results has been reported by other researchers [49,50].

3.2.2. Flexural Strength

The test for flexural strength was conducted using a three-point loading system on prism specimens cured for 7 and 28 days. The results presented in Figure 8 are an average of three specimens produced for each mixture. From the results, the addition of low-grade calcined clay alone in percentages up to 40% caused a reduction in the flexural strength at both 7 and 28 days. The flexural strength losses at 7 days were 4.8%, 14.3%, 15.7%, and 23.8%, respectively, lower than the reference specimen. At 28 days, the results obtained for 10CC, 20CC, 30CC, and 40CC trailed the reference specimen by 0.4%, 2.6%, 5.7%, and 18.9%, respectively. The lower rate of strength development at 7 days was due to the characteristics of the calcined clay, which almost behaved as an inert material in the concrete mixture due to its slow reactivity at early ages [51]. The low kaolinite content of the clay impacted its metakaolinite composition after calcination, which eventually affected pozzolanic reactivity [52]. This reactivity, however, greatly improved at 28 days, but was not enough to overcome the effect of dilution at all replacement levels.

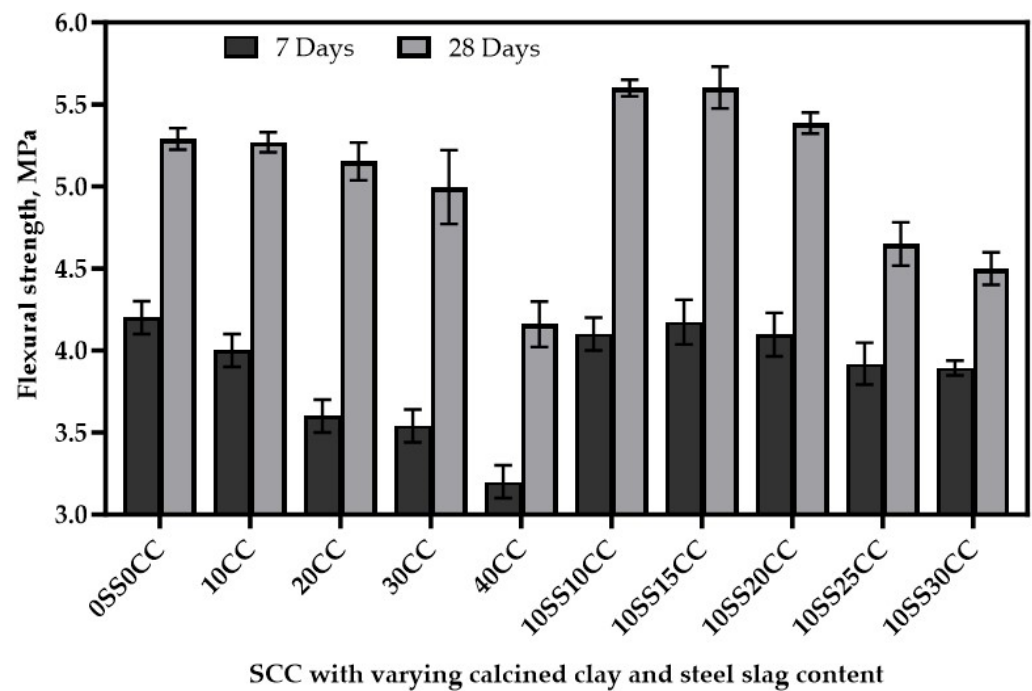


Figure 8. Flexural strength of SCC.

Similar to the compressive strength, the flexural strength achieved a significant improvement when the binary mixture containing calcined clay was doped with 10% steel slag. At a curing age of 28 days, the interaction between the constituents of the steel slag and calcined clay caused the specimens 10SS10CC, 10SS15CC, and 10SS20CC to obtain flexural strengths which were 5.5%, 5.6%, and 1.8%, respectively, greater than the reference concrete. This was due to the synergistic influence of the strong reaction between the alumina phases in the Portland cement with the steel slag–calcined clay blend, as reported by Sujjavanich et al. [50]. Again, the synergistic filling of voids by the steel slag–calcined clay particles produced a relatively denser structure, which translated into strength [53]. The

influence of steel slag in 10SS25CC and 10SS30CC could not match the dilution effect [54] caused by the 35% and 40% total pozzolan infiltration, thereby compromising the flexural strength by 13.8% and 14.9%, respectively. This observation is consistent with the literature, which confirms the slow reactivity of pozzolans at early ages and the active consumption of portlandite at later ages to produce further cementitious compounds, improving strength [55].

3.3. XRD Analysis of Hydrated SCC

Phase identification of the blended cement paste mixtures containing calcined clay and steel slag was conducted using XRD analysis. After 28 days of curing, the samples were crushed and ground in an agate mortar into fine powder. The powdered sample was subsequently used for the XRD study. Figure 9 presents the XRD patterns of all the SCC mixtures. The dominant phases present include calcite, quartz, anorthite, and portlandite. Portlandite [Ca(OH)₂] is seen at the diffraction peak with a 2θ angle of 16.5° and 33.3°. There was a significant reduction in the peak heights of portlandite in the mixtures containing steel slag and calcined clay, irrespective of their percentage replacement. The most significant reduction was found in the mixtures containing 10% steel slag and 10% calcined clay (10SS10CC) and 10% steel slag and 15% calcined clay (10SS15CC). Thus, it can be concluded that some of the portlandite produced during the hydration reaction was depleted by its pozzolanic reactivity with the steel slag and calcined clay, which can improve the microstructure of the concrete matrix by creating further calcium silicate hydrate gel and subsequently leading to strength improvement, as seen in Figures 8–10. This is in line with results reported by other researchers [50,56].

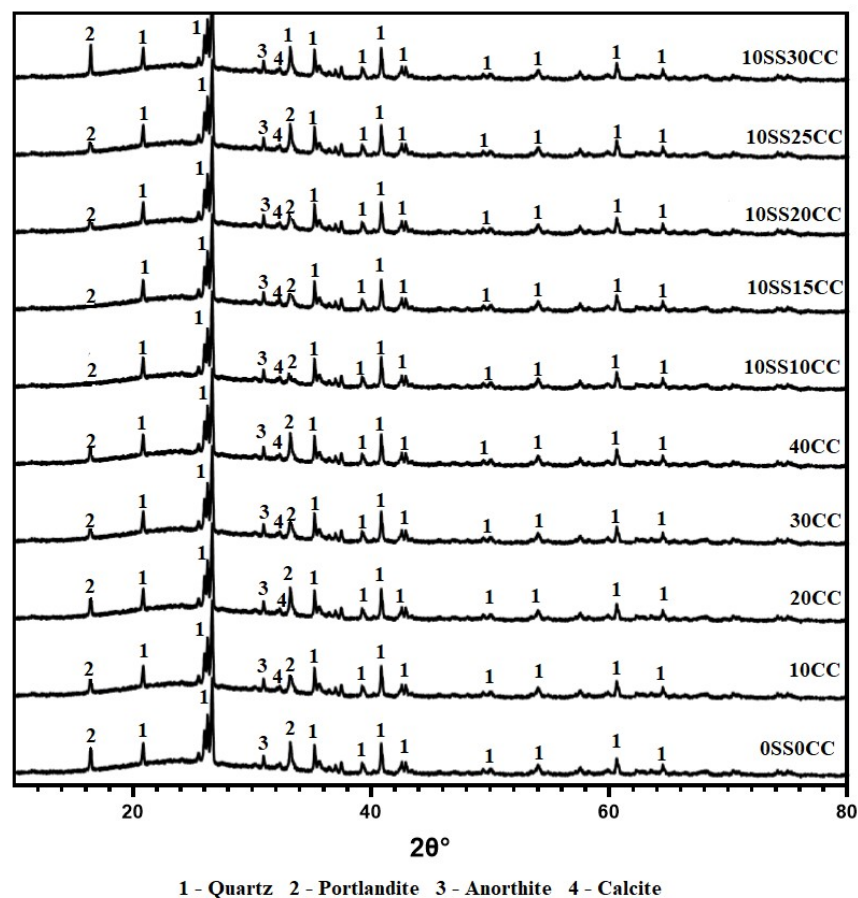


Figure 9. XRD patterns of 28-day hydrated SCC containing calcined clay and steel slag.

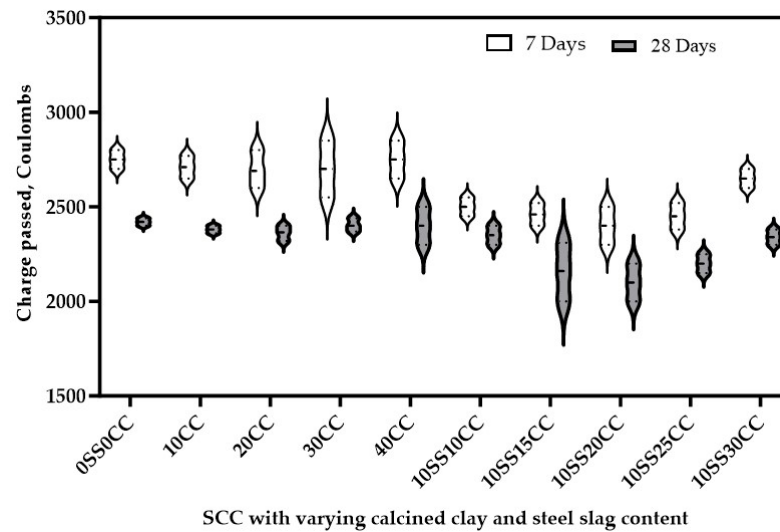


Figure 10. Chloride permeability of SCC.

3.4. Chloride Ingress Resistance

The overall charge passed in the RCPT provides an indirect estimation of the concrete’s resistance to chloride ions. A higher resistance to chloride infiltration is implied by a lower charge passed. Although the test has drawn a few critiques, it is still commonly used in global construction practises to assess the quality of concrete, particularly concrete’s resistance to chlorides. The validity of this test method for assessing the chloride resistance of concretes containing SCM’s was stressed, once again, in a recent investigation [57]. Figure 10 shows the experimental data of the SCC after 7 and 28 days of curing. From the results, the concrete containing calcined clay and steel slag obtained a minimum amount of charge passed at 7 and 28 days. This demonstrates an exceptional resistance to chloride ions at both early and later ages. However, the resistance at 28 days was found to be greater than that at 7 days. According to the ASTM 1202 concrete classification, the quality of concrete containing pozzolans is significantly improved only after longer periods of curing. All the blended cement concrete samples, irrespective of the various admixture combinations, offered a better chloride resistance than the reference cement concrete (which is still considered to be moderate). Additionally, calcined clay has a higher concentration of reactive aluminates, which can result in a higher chloride binding rate as compared to other systems because of the different hydration products [58].

3.5. Sulphate Resistance

Self-compacting concrete samples were subjected to a sodium sulphate environment and were evaluated for weight loss, physical changes, and compressive strength variations. There was no spalling, cracking, or deterioration observed on the concrete after visual inspection. In Figure 11, a relationship between these impacts is also depicted. It is seen that a 5% Na₂SO₄ environment had a negative impact on the weight and ensuing compressive strength of the self-compacting concrete. The highest losses were found in the reference sample. Generally, all the blended cement samples performed appreciably in resisting the sulphate attack. A direct relation was seen to exist between weight loss and strength loss. As the weight of the samples decreased, the compressive strength decreased with an R² value of 0.9746, signifying a good fit. The performance of the concrete containing steel slag and calcined clay was due to the low porosity of the blended cement concrete, confirmed in the chloride permeability test results in Figure 10 and consistent with the works of previous researchers [59]. The addition of the two pozzolans contributed to the refinement of the pore structure within the concrete matrix. This refinement impeded the ingress of aggressive sulphate ions into the concrete matrix, limiting their interaction with the cementitious phases and mitigating the detrimental effects of sulphate attack. Also, the

finer particle sizes of the calcined clay and steel slag improved packing within the concrete mixture, resulting in a denser microstructure, which reduced capillarity and permeability, restricting the movement of sulphate ions through the concrete matrix. The resistance of the cement samples to sulphate attack is shown in Table 3.

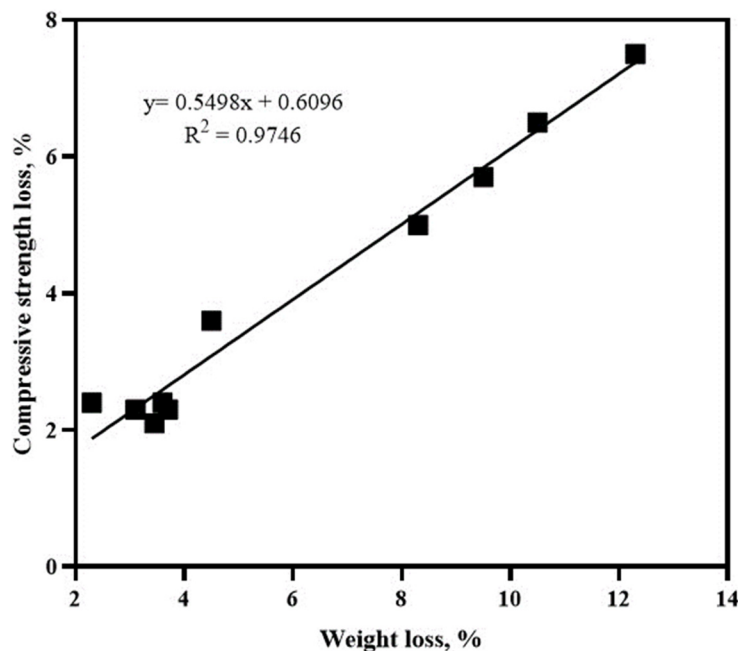


Figure 11. Relation between weight loss and compressive strength loss after subjecting the SCC to 5% Na₂SO₄ environment for 90 days.

Table 3. Weight and compressive strength loss after sulphate attack.

Sample	Weight Loss, %	Strength Loss, %
0SS0CC	12.3	7.5
10CC	10.5	6.5
20CC	9.5	5.7
30CC	8.3	5
40CC	4.5	3.6
10SS10CC	3.6	2.4
10SS15CC	3.45	2.1
10SS20CC	3.7	2.3
10SS25CC	3.1	2.3
10SS30CC	2.3	2.4

4. Conclusions

This study investigated the use of ternary blended calcined clay and steel slag as alternative binders and their effect on the rheology, mechanical strength development, and durability properties of self-compacting concrete. The following conclusions were drawn from an analysis of the results:

1. All blends showed a good consistency and workability. Steel slag effectively compensated for the decrease in fluidity caused by the addition of calcined clay. Mixtures containing 10% and 10/15% calcined clay showed optimal performances in achieving desirable fresh SCC properties.
2. After 28 days, the specimens 10SS10CC, 10SS15CC, and 10SS20CC achieved compressive strengths approximately 6.2%, 3.5%, and 3.9% higher than the reference sample. Except for sample 10SS30CC, which lagged behind the reference specimen, all mixtures containing steel slag exhibited flexural strengths higher than the reference SCC.

3. Concrete containing calcined clay and steel slag obtained a minimum amount of charge passed at 7 and 28 days. This demonstrates an exceptional resistance to chloride ions at both early and later ages.
4. The XRD analysis revealed a significant decrease in the peak heights of portlandite in mixtures containing steel slag and calcined clay, regardless of their replacement percentage. From the XRD analysis, there were significant reductions in the peak heights of portlandite in mixtures containing steel slag and calcined clay, irrespective of their percentage replacement. The most significant reduction was found in mixtures containing 10% steel slag and 10% calcined clay (10SS10CC) and 10% steel slag and 15% calcined clay (10SS15CC).
5. Overall, the blended cement samples exhibited higher performances in resisting the sulphate attack. A direct relation was seen to exist between weight loss and strength loss due to sulphate attack. As the weight of the samples decreased, the compressive strength decreased.

The incorporation of calcined clays and steel slag in concrete could enhance sustainability by reducing reliance on traditional cement, thereby decreasing the carbon emissions associated with cement production. Further studies into the long-term durability of these concrete mixtures are recommended.

Author Contributions: Conceptualization, M.K.; methodology, M.K. and K.B.; software, M.K. and K.B.; validation, M.K.; formal analysis, M.K. and K.B.; investigation, K.B. and M.K.; resources, M.K. and K.B.; data curation, K.B. and M.K.; writing—original draft preparation, K.B.; writing—review and editing, M.K.; visualization, M.K.; supervision, M.K.; project administration, M.K.; funding acquisition, M.K. and K.B. All authors have read and agreed to the published version of the manuscript.

Funding: This research received no external funding, and the APC was funded by MDPI open access publishing in Basel/Switzerland.

Data Availability Statement: Data are contained within the article.

Conflicts of Interest: The authors declare no conflict of interest.

References

1. Madandoust, R.; Mousavi, S.Y. Fresh and hardened properties of self-compacting concrete containing metakaolin. *Constr. Build. Mater.* **2012**, *35*, 752–760. [[CrossRef](#)]
2. Sobuz, M.H.; Meraz, M.M.; Safayet, M.A.; Mim, N.J.; Mehedi, M.T.; Farsangi, E.N.; Shrestha, R.K.; Arafin, S.A.; Bibi, T.; Hussain, M.S.; et al. Performance evaluation of high-performance self-compacting concrete with waste glass aggregate and metakaolin. *J. Build. Eng.* **2023**, *67*, 105976. [[CrossRef](#)]
3. Jain, A.; Gupta, R.; Chaudhary, S. Sustainable development of self-compacting concrete by using granite waste and fly ash. *Constr. Build. Mater.* **2020**, *262*, 120516. [[CrossRef](#)]
4. Pravitha, J.J.; Merina, R.N.; Subash, N. Mechanical properties and microstructural characterization of ferrock as CO₂-negative material in self-compacting concrete. *Constr. Build. Mater.* **2023**, *396*, 132289. [[CrossRef](#)]
5. Jain, A.; Gupta, R.; Chaudhary, S. Performance of self-compacting concrete comprising granite cutting waste as fine aggregate. *Constr. Build. Mater.* **2019**, *221*, 539–552. [[CrossRef](#)]
6. Choudhary, S.; Chaudhary, S.; Jain, A.; Gupta, R. Valorization of waste rubber tyre fiber in functionally graded concrete. *Mater. Today Proc.* **2020**, *32*, 645–650. [[CrossRef](#)]
7. Nilimaa, J. Smart materials and technologies for sustainable concrete construction. *Dev. Built Environ.* **2023**, *15*, 100177. [[CrossRef](#)]
8. Mim, N.J.; Meraz, M.M.; Islam, M.H.; Farsangi, E.N.; Mehedi, M.T.; Arafin, S.A.; Shrestha, R.K. Eco-friendly and cost-effective self-compacting concrete using waste banana leaf ash. *J. Build. Eng.* **2023**, *64*, 105581. [[CrossRef](#)]
9. Wee, J. A review on carbon dioxide capture and storage technology using coal fly ash. *Appl. Energy* **2013**, *106*, 143–151. [[CrossRef](#)]
10. Boakye, K.; Khorami, M. Hydration, Reactivity and Durability Performance of Low-Grade Calcined Clay-Silica Fume Hybrid Mortar. *Appl. Sci.* **2023**, *13*, 11906. [[CrossRef](#)]
11. Scrivener, K.; Martirena, F.; Bishnoi, S.; Maity, S. Calcined clay limestone cements (LC3). *Cem. Concr. Res.* **2018**, *114*, 49–56. [[CrossRef](#)]
12. Avet, F.; Scrivener, K. Investigation of the calcined kaolinite content on the hydration of Limestone Calcined Clay Cement (LC3). *Cem. Concr. Res.* **2018**, *107*, 124–135. [[CrossRef](#)]
13. Sarfo-Ansah, J.; Atiemo, E.; Bediako, M.; Tagbor, T.A.; Boakye, K.A.; Adjei, D. The influence of calcined clay pozzolan, low-CaO steel slag and granite dust on the alkali-silica reaction in concrete. *J. Eng. Res. Appl.* **2015**, *5*, 19–27.

14. Tironi, A.; Trezza, M.A.; Scian, A.N.; Irassar, E.F. Assessment of pozzolanic activity of different calcined clays. *Cem. Concr. Compos.* **2013**, *37*, 319–327. [[CrossRef](#)]
15. Msinjili, N.S.; Vogler, N.; Sturm, P.; Neubert, M.; Schröder, H.-J.; Kühne, H.-C.; Hüniger, K.-J.; Gluth, G.J. Calcined brick clays and mixed clays as supplementary cementitious materials: Effects on the performance of blended cement mortars. *Constr. Build. Mater.* **2021**, *266*, 120990. [[CrossRef](#)]
16. Alujas, A.; Fernández, R.; Quintana, R.; Scrivener, K.L.; Martirena, F. Pozzolanic reactivity of low grade kaolinitic clays: Influence of calcination temperature and impact of calcination products on OPC hydration. *Appl. Clay Sci.* **2015**, *108*, 94–101. [[CrossRef](#)]
17. Boakye, K.; Khorami, M. Impact of low-reactivity calcined clay on the performance of fly ash-based geopolymer mortar. *Sustainability* **2023**, *15*, 13556. [[CrossRef](#)]
18. Sarfo-Ansah, J.; Atiemo, E.; Boakye, K.; Adjei, D.; Adjaottor, A. Calcined Clay Pozzolan as an Admixture to Mitigate the Alkali-Silica Reaction in Concrete. *J. Mater. Sci. Chem. Eng.* **2014**, *2*, 20–26. [[CrossRef](#)]
19. Hay, R.; Celik, K. Performance enhancement and characterization of limestone calcined clay cement (LC3) produced with low-reactivity kaolinitic clay. *Constr. Build. Mater.* **2023**, *392*, 131831. [[CrossRef](#)]
20. Bouchenafa, O.; Hamzaoui, R.; Bennabi, A.; Colin, J. PCA effect on structure of fly ashes and slag obtained by mechano-synthesis. Applications: Mechanical performance of substituted paste CEMI 50% slag/or fly ashes. *Constr. Build. Mater.* **2019**, *203*, 120–133. [[CrossRef](#)]
21. Piemonti, A.; Conforti, A.; Cominoli, L.; Sorlini, S.; Luciano, A.; Plizzari, G. Use of iron and steel slags in concrete: State of the art and future perspectives. *Sustainability* **2021**, *13*, 556. [[CrossRef](#)]
22. Wang, Q.; Yan, P.; Mi, G. Effect of blended steel slag–GBFS mineral admixture on hydration and strength of cement. *Constr. Build. Mater.* **2012**, *35*, 8–14. [[CrossRef](#)]
23. Diao, Z.K.; Pan, Z.H.; Ma, J.; Gao, Z.; Qiu, T. Experimental study on workability and compressive strength of self-compacting concrete with recycled aggregate of steel slag. *Build. Struct.* **2016**, *46*, 52–55.
24. Atiemo, E.; Boakye, K.A.; Sarfo-Ansah, J. Hydration and mechanical properties of Portland cement blended with Low-CaO Steel Slag. *J. Phys. Sci. Appl.* **2014**, *4*, 444–449.
25. Wang, M.; Xie, Y.; Long, G.; Ma, C.; Zeng, X.; Qiang, F. The impact mechanical characteristics of steam-cured concrete under different curing temperature conditions. *Constr. Build. Mater.* **2020**, *241*, 118042. [[CrossRef](#)]
26. Devi, V.S.; Kumar, M.M.; Iswarya, N.; Gnanavel, B.K. Durability of steel slag concrete under various exposure conditions. *Mater. Today Proc.* **2020**, *22*, 2764–2771. [[CrossRef](#)]
27. Khatib, J.M.; Hibbert, J.J. Selected engineering properties of concrete incorporating slag and metakaolin. *Constr. Build. Mater.* **2005**, *19*, 460–472. [[CrossRef](#)]
28. Sullivan, M.S.; Chorzepa, M.G.; Durham, S.A. Characterizing the performance of ternary concrete mixtures involving slag and metakaolin. *Infrastructures* **2020**, *5*, 14. [[CrossRef](#)]
29. Singh, S.K.; Tiwari, N.; Jyoti. Development of sustainable ternary cementitious binder with OPC integrating calcined clay and LF slag. *J. Build. Eng.* **2023**, *75*, 107025. [[CrossRef](#)]
30. British Standards Institution. *BS EN 197-1; 2011-Cement—Composition, Specifications and Conformity Criteria for Common Cements*. British Standards Institution: Milton Keynes, UK, 2019.
31. EFNARCF. *Specification and Guidelines for Self-Compacting Concrete*; European Federation of Specialist Construction Chemicals and Concrete System: Farnham, UK, 2002.
32. *ASTM C109/C109M*; Standard Test Method for Compressive Strength of Hydraulic Cement Mortars (Using 2-in. or 50 mm Cube Specimens). ASTM International: West Conshohocken, PA, USA, 2002.
33. *ASTM C78/C78M-18*; Standard Test Method for Flexural Strength of Concrete Using Simple Beam with Third-Point Loading. ASTM International: West Conshohocken, PA, USA, 2018.
34. Ramezani-pour, A.A.; Pilvar, A.; Mahdikhani, M.; Moodi, F. Practical evaluation of relationship between concrete resistivity, water penetration, rapid chloride penetration and compressive strength. *Constr. Build. Mater.* **2011**, *25*, 2472–2479. [[CrossRef](#)]
35. Güneyisi, E.; Gesoğlu, M. Properties of self-compacting mortars with binary and ternary cementitious blends of fly ash and metakaolin. *Mater. Struct.* **2008**, *41*, 1519–1531. [[CrossRef](#)]
36. Karthiga@Shenbagam, N.; Arun Siddharth, M.; Kannan, V.; Dhanusree, C. Experimental investigation of self-compacting concrete (SCC) using fly ash. *Mater. Today Proc.* **2023**, *in press*. [[CrossRef](#)]
37. Güneyisi, E.; Gesoğlu, M.; Al-Goody, A.; İpek, S. Fresh and rheological behavior of nano-silica and fly ash blended self-compacting concrete. *Constr. Build. Mater.* **2015**, *95*, 29–44. [[CrossRef](#)]
38. Barkat, A.; Kenai, S.; Menadi, B.; Kadri, E.; Soualhi, H. Effects of local metakaolin addition on rheological and mechanical performance of self-compacting limestone cement concrete. *J. Adhes. Sci. Technol.* **2019**, *33*, 963–985. [[CrossRef](#)]
39. Al-Oran, A.A.A.; Safiee, N.A.; Nasir, N.A.M. Fresh and hardened properties of self-compacting concrete using metakaolin and GGBS as cement replacement. *Eur. J. Environ. Civ. Eng.* **2022**, *26*, 379–392. [[CrossRef](#)]
40. Sfikas, I.P.; Badogiannis, E.G.; Trezos, K.G. Rheology and mechanical characteristics of self-compacting concrete mixtures containing metakaolin. *Constr. Build. Mater.* **2014**, *64*, 121–129. [[CrossRef](#)]
41. Badogiannis, E.G.; Sfikas, I.P.; Voukia, D.V.; Trezos, K.G.; Tsvilis, S.G. Durability of metakaolin Self-Compacting Concrete. *Constr. Build. Mater.* **2015**, *82*, 133–141. [[CrossRef](#)]

42. Boakye, K.; Khorami, M.; Saidani, M.; Ganjian, E.; Dunster, A.; Ehsani, A.; Tyrer, M. Mechanochemical characterisation of calcined impure kaolinitic clay as a composite binder in cementitious mortars. *J. Compos. Sci.* **2022**, *6*, 134. [[CrossRef](#)]
43. Dixit, A.; Du, H.; Pang, S.D. Marine clay in ultra-high performance concrete for filler substitution. *Constr. Build. Mater.* **2020**, *263*, 120250. [[CrossRef](#)]
44. Wild, S.; Khatib, J.M.; Jones, A. Relative strength, pozzolanic activity and cement hydration in superplasticised metakaolin concrete. *Cem. Concr. Res.* **1996**, *26*, 1537–1544. [[CrossRef](#)]
45. Hasan, Z.A.; Nasr, M.S.; Abed, M.K. Properties of reactive powder concrete containing different combinations of fly ash and metakaolin. *Mater. Today Proc.* **2021**, *42*, 2436–2440. [[CrossRef](#)]
46. Saboo, N.; Shivhare, S.; Kori, K.K.; Chandrappa, A.K. Effect of fly ash and metakaolin on pervious concrete properties. *Constr. Build. Mater.* **2019**, *223*, 322–328. [[CrossRef](#)]
47. Vance, K.; Aguayo, M.; Oey, T.; Sant, G.; Neithalath, N. Hydration and strength development in ternary portland cement blends containing limestone and fly ash or metakaolin. *Cem. Concr. Compos.* **2013**, *39*, 93–103. [[CrossRef](#)]
48. Moser, R.D.; Jayapalan, A.R.; Garas, V.Y.; Kurtis, K.E. Assessment of binary and ternary blends of metakaolin and Class C fly ash for alkali-silica reaction mitigation in concrete. *Cem. Concr. Res.* **2010**, *40*, 1664–1672. [[CrossRef](#)]
49. Boakye, K.; Khorami, M. Influence of Calcined Clay Pozzolan and Aggregate Size on the Mechanical and Durability Properties of Pervious Concrete. *J. Compos. Sci.* **2023**, *7*, 182. [[CrossRef](#)]
50. Sujavanich, S.; Suwanvitaya, P.; Chaysuwan, D.; Heness, G. Synergistic effect of metakaolin and fly ash on properties of concrete. *Constr. Build. Mater.* **2017**, *155*, 830–837. [[CrossRef](#)]
51. Fernandez, R.; Martirena, F.; Scrivener, K.L. The origin of the pozzolanic activity of calcined clay minerals: A comparison between kaolinite, illite and montmorillonite. *Cem. Concr. Res.* **2011**, *41*, 113–122. [[CrossRef](#)]
52. Fan, Y.; Zhang, S.; Kawashima, S.; Shah, S.P. Influence of kaolinite clay on the chloride diffusion property of cement-based materials. *Cem. Concr. Compos.* **2014**, *45*, 117–124. [[CrossRef](#)]
53. Garg, R.; Garg, R.; Eddy, N.O.; Khan, M.A.; Khan, A.H.; Alomayri, T.; Berwal, P. Mechanical strength and durability analysis of mortars prepared with fly ash and nano-metakaolin. *Case Stud. Constr. Mater.* **2023**, *18*, e01796. [[CrossRef](#)]
54. Li, J.; Zhang, W.; Li, C.; Monteiro, P.J.M. Eco-friendly mortar with high-volume diatomite and fly ash: Performance and life-cycle assessment with regional variability. *J. Clean. Prod.* **2020**, *261*, 121224. [[CrossRef](#)]
55. Skibsted, J.; Snellings, R. Reactivity of supplementary cementitious materials (SCMs) in cement blends. *Cem. Concr. Res.* **2019**, *124*, 105799. [[CrossRef](#)]
56. Shen, P.; Lu, L.; Chen, W.; Wang, F.; Hu, S. Efficiency of metakaolin in steam cured high strength concrete. *Constr. Build. Mater.* **2017**, *152*, 357–366. [[CrossRef](#)]
57. Dhanya, B.S.; Santhanam, M. Performance evaluation of rapid chloride permeability test in concretes with supplementary cementitious materials. *Mater. Struct.* **2017**, *50*, 67. [[CrossRef](#)]
58. Dhandapani, Y.; Sakthivel, T.; Santhanam, M.; Gettu, R.; Pillai, R.G. Mechanical properties and durability performance of concretes with Limestone Calcined Clay Cement (LC3). *Cem. Concr. Res.* **2018**, *107*, 136–151. [[CrossRef](#)]
59. Rossetti, A.; Ikumi, T.; Segura, I.; Irassar, E.F. Sulfate performance of blended cements (limestone and illite calcined clay) exposed to aggressive environment after casting. *Cem. Concr. Res.* **2021**, *147*, 106495. [[CrossRef](#)]

Disclaimer/Publisher’s Note: The statements, opinions and data contained in all publications are solely those of the individual author(s) and contributor(s) and not of MDPI and/or the editor(s). MDPI and/or the editor(s) disclaim responsibility for any injury to people or property resulting from any ideas, methods, instructions or products referred to in the content.